

# CAAPI – Over-Expression of Iturin A to Combat Coffee Leaf Rust

Akshay Ajit Parmar<sup>1</sup>, Angela Anna Jossy<sup>1</sup>, Anirudh Saravanan<sup>1</sup>, C Hita Poonacha<sup>1</sup>, Harini G Karthik<sup>1</sup>, I A Ganit Cariappa<sup>1</sup>, Jalla Varshith<sup>1</sup>, Karan Sanjay<sup>1</sup>, Kaushika Ganapathi Venkataraman<sup>1</sup>, Lavanya Dalmia<sup>1</sup>, Mihika Chitre<sup>1</sup>, Muhammad Zaid Hassan<sup>1</sup>, Navya Subramanian Anantharaman<sup>1</sup>, Nithya Swarandika Sappani<sup>1</sup>, Ram P Shetty<sup>1</sup>, Rhea Sridhar Nadig<sup>1</sup>, Sania Serrao<sup>1</sup>, Shyaam Shashidhar Haridas<sup>1</sup>, Tanaya Sengupta<sup>1</sup>, Vengala Deepali<sup>1</sup>, Vignesh Vijaysekhar<sup>1</sup>

<sup>1</sup>Team MIT-MAHE, Manipal Institute of Technology, India

**Abstract**—Coffee leaf rust (caused by *Hemileia vastatrix*) is a fungal disease that inflicts significant yield losses to global *Coffea arabica* production. Conventional fungicides negatively impact the environment, highlighting the need for sustainable solutions. In this study, we enhance the antifungal capabilities of *Bacillus subtilis* ATCC 13952 by increasing Iturin A production during exponential and stress-induced stationary phases. The native promoter of the Iturin A operon ( $P_{itu}$ ) was replaced with a stronger promoter ( $P_{43}$  and  $P_{bacA}$ ) through homologous recombination. A dual promoter system was also designed to improve the efficiency of Iturin A production. Biochemical assays and High-Performance Liquid Chromatography (HPLC) analyses were used to study and quantify Iturin production. Computational modelling and molecular dynamics simulations were performed to test the strength of the engineered promoters.

This approach will be implemented in a wettable powder formulation containing a kill switch to prevent the unintended spread of the genetically modified organism. A machine learning model (BREW) was developed to accurately predict coffee yields based on various environmental parameters, offering farmers crucial insights for better crop management.

**Keywords**—Coffee leaf rust, *Hemileia vastatrix*, *Bacillus subtilis*, promoter replacement, homologous recombination

## I. INTRODUCTION

Coffee leaf rust (CLR), caused by the fungus *Hemileia vastatrix*, poses a significant threat to *Coffea arabica*, the species responsible for most global coffee production. CLR incurs up to \$1 billion in annual losses and reduces coffee yields by up to 75%, severely impacting farmers' livelihoods. The disease spreads through urediniospores that invade coffee leaves, leading to premature defoliation and weakened plants. Urediniospores germinate on the underside of the leaf showing visible orange spots on the leaf surface within 2 weeks of primary infection, as a marker that infection has spread. With 2.5 billion cups of coffee consumed daily, CLR not only jeopardizes the livelihoods of millions of farmers but also threatens the economies of coffee-exporting countries. Traditional chemical fungicides used against CLR cause

environmental harm, highlighting the need for sustainable alternatives.

Our project aims to address CLR by enhancing the production of Iturin A, an antifungal lipopeptide produced by *Bacillus subtilis*.

The Iturin A operon is 38kb long and consists of four genes: *ItuD*, *ItuA*, *ItuB*, and *ItuC*, each encoding their respective enzymes. *ItuA* is a hybrid polyketide synthetase (PKS) and non-ribosomal peptide synthetase (NRPS), while the others (*ItuB*, *ItuC*) are NRPSs [1]. Each NRPS has modules that function as catalytic units by incorporating one amino acid into the growing peptide chain [2], [3]. The lipopeptide assembly begins with *ItuA* where the acyl-CoA ligase domain activates a fatty acid, followed by *ItuD* catalyzing a reaction with malonyl-CoA. The growing peptide chain progresses through *ItuB* and *ItuC*, incorporating amino acids via adenylation, condensation, and epimerization. The thioesterase domain then cleaves and cyclizes the final lipopeptide.

Out of the multiple potential methods reviewed for increase in expression rates, promoter replacement was the most reliable option. Thus, we turned our attention towards the selection and construction of a suitable promoter to replace  $P_{itu}$ , the natural promoter of Iturin A.

Certain aspects that needed to be kept in mind while trying to overproduce such a molecule are: (i) increase in metabolic load that would decrease the bacterial lifespan [4]. (ii) Iturin A is naturally produced only during its stationary phase of growth [5]. (iii) To ensure that Iturin is produced when in proximity to a fungus or stress inducing factor, its trigger pathway needs to be conserved as the natural promoter is activated by stress.

Keeping all these points in mind,  $P_{itu}$  will be replaced with a more potent promoter using homologous recombination in our host strain *Bacillus Subtilis* ATCC 13952. This approach will allow us to significantly increase the production of Iturin A without the need to transfer the operon into a bacterial plasmid, which would be impractical due to its size and complexity.

To enhance Iturin production, we also proposed a dual-promoter system by combining the two most effective promoters mined through literature review.

## II. Materials and Methods

### A. Chemicals, Bacterial Strains, and Experimental Conditions

The *Bacillus subtilis* ATCC 13952 strain was procured from the American Type Culture Collection (ATCC). All chemicals used were of analytical grade. High Performance Liquid Chromatography (HPLC) analysis utilized a Shimadzu system with a C18 column and HPLC-grade solvents (0.1% TFA in water). HPLC-grade methanol and acetonitrile were sourced from Sigma-Aldrich (St. Louis, MO, USA). Hydrochloric acid (6 M), sodium hydroxide (1 M), and potassium chloride (3 M) solutions were prepared in distilled water for pH calibration and adjustments. Crystal violet, Gram's iodine, 95% ethanol, safranin, and malachite green stains were employed for staining assays. Indole testing utilized Kovac's reagent, while methyl red indicator and Barritt's A and B reagents were used for MR-VP assays. Growth curve analysis was performed in Luria-Bertani (LB) broth media at 37°C and 200 rpm. Iturin extraction used Potato Dextrose Broth (PDB) and LB broth and involved acid-base treatments with 6 M HCl, 1M NaOH, and methanol, employing a magnetic stirrer, centrifuge, sterile filtration processes. Homologous recombination experiments used *Bacillus subtilis* cells, linear DNA fragment containing green fluorescence protein (GFP) as the selectable marker, recovery media, and a 37°C incubator. Gibson assembly reactions included PCR-amplified DNA fragments, and competent *Bacillus subtilis* cells. GFP detection involved LB medium and gel docking. PCR was conducted and verified, using Taq DNA polymerase, dNTPs, primers, Thermocycler and agarose gel electrophoresis reagents, and the QIAprep Spin Miniprep Kit. All solutions and media were sterilized by autoclaving at 121°C for 20 minutes unless specified otherwise.

### B. Homologous Recombination in *Bacillus subtilis*

Homologous recombination (HR) is a method for modifying bacterial genomes by replacing or inserting specific DNA sequences with flanking homologous regions. In this project, HR employed to enhance Iturin A production in *Bacillus subtilis* by replacing the native  $P_{itu}$  promoter with a stronger promoter,  $P_{43}$  and  $P_{bacA}$ , to improve gene expression during both exponential and stationary phases of growth [6]. The process involves several key steps:

1. **Designing the DNA Insert**
2. **Recognition of a Double-Strand Break (DSB)**
3. **End Processing and Strand Invasion**
4. **DNA Synthesis and Ligation**
5. **Resolution of the Holliday Junction** [7], [8]
6. **Validation of HR through the selectable marker i.e., GFP** [9].

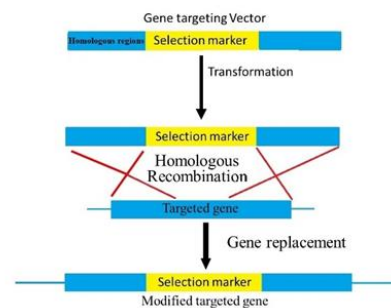


Fig 1: Homologous Recombination

$P_{43}$  promoter + green fluorescent protein with homologous flanks

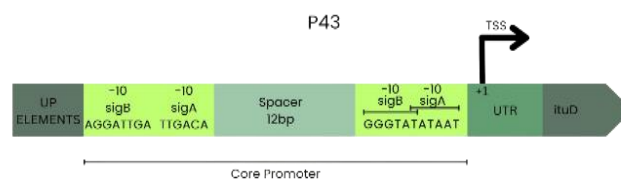


Fig 2:  $P_{43}$  HR fragment

$P_{bacA}$  promoter + GFP with homologous flanks.

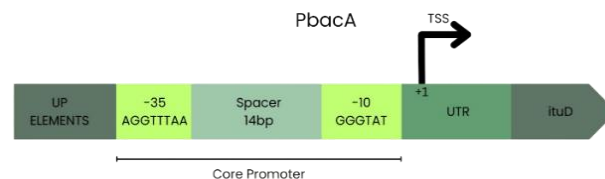


Fig 3:  $P_{bacA}$  HR fragment

To study the difference in the homologous recombination success rate, the  $P_{bacA}$  construct (as in Fig. 3), had 350bp of homologous flanks while the  $P_{43}$  construct (as in Fig. 2) had 500bp.

A longer homology fragment will increase the size of the linear fragment which will cause the construct to be unstable whereas a smaller homology length will decrease the chances of HR. Through our research it was found that different papers recommended different homology lengths for successful HR, hence, constructing two fragments with different homology lengths was essential to our understanding of the HR process.

### C. Primer Design

The primers for  $P_{bacA}$  and  $P_{43}$  were designed with attention to detail. Their design process involved a thorough consideration of multiple critical parameters to ensure optimal performance and compatibility for PCR and Gibson assembly.

Table 1: Primer Data Sheet

Fragment	Primer	Primer Sequence (5'-3')	Number of Bases	GC Content	Tm value (°C)
<i>P<sub>bacA</sub></i>	Forward	CGCCGCTTAC AAGTGTAAC	19	55	59.3
	Reverse	GACGGTTTC AAGGAATTT ACG	22	41.7	59.3
<i>P<sub>43</sub></i>	Forward	CACAGCTTG CCGGTGTC	17	43	58
	Reverse	GGGGGCTTC ACAATGATTT ATG	23	45.5	58

#### D. Growth Curve

To analyze the growth pattern, 6-hour and 24-hour growth curve experiments were conducted. For both experiments, an overnight culture was prepared containing LB broth at the required pH with *B. subtilis* and incubating it at 37°C and rotated at 180–200 rpm for 12 hours to reach the stationary phase. The broth was inoculated with 2% of overnight culture and left to incubate till the optimum OD was reached.

For the 6-hour growth curve, a 1:500 dilution was prepared using the 2% culture. The flask was incubated at 37°C and rotated at 200-250 rpm. To measure the growth of the bacteria, 1000 µL of the bacterial cultures were transferred to a 10mm plastic cuvette. The cuvette was placed in a UV/Vis spectrophotometer (Eppendorf) to monitor the OD at 600 nm of the bacteria. The OD of the flasks were read every 30 minutes for 6 hours.

For the 24-hour growth curve, a similar setup was used; however, measurements were taken at hourly intervals for the first 12 hours and at 2-hour intervals for the subsequent 12 hours using flasks prepared on the previous day. The recorded values were plotted against time to generate growth curves, allowing visualization of the lag, log, stationary, and death phases.

#### E. Confirmatory tests

Various staining and biochemical tests analyzed the physiological and metabolic traits of *Bacillus subtilis*. Gram staining involved crystal violet, Gram's iodine as a mordant, ethanol for decolorization, and safranin as a counterstain. Hot spore staining detected endospores, using malachite green with heat for spores and safranin for vegetative cells.

Biochemical tests included the indole test, methyl red (MR) test, and Voges-Proskauer (VP) test. The indole test, performed by adding Kovac's reagent to the culture, is conducted to detect tryptophan metabolism. The MR test was used to assess acid production from glucose fermentation by introducing Methyl Red indicator to an inoculated broth after incubation. The VP

test, conducted on the same culture, determined the production of neutral end products through the addition of Barritt's reagents.

#### F. HPLC

HPLC was performed to quantify the Iturin A produced by our strain *Bacillus subtilis* ATCC 13952 (*Supplementary 2*).

The system was flushed with water and acetonitrile to remove air bubbles before use.

For method development, 100µL of each diluted sample was loaded onto the autosampler. The 12.5µg/mL concentration was chosen for initial tests, with additional runs using 25µg/mL to ensure the instrument could detect higher iturin A levels. Multiple combinations of mobile phase solvents, flow rates (0.8mL/min and 1mL/min), and parameters were tested.

After several iterations (*Supplementary 2*), the optimal conditions for peak separation were found: a 40-80% acetonitrile gradient, a flow rate of 0.8mL/min, a column temperature of 25°C, and a pressure gradient corresponding to the mobile phase. These conditions were finalized for the ideal method file for iturin A analysis.

HPLC runs were conducted using methanol as the blank. HPLC was performed for the test samples, i.e., extracted Iturin A in both LB broth and PDB using the above-mentioned optimal parameters.

### III. RESULTS

#### A. Confirmatory Tests



Fig 4: Gram Staining

*Bacillus subtilis* ATCC 13952 was confirmed as a Gram-positive bacterium with rod-shaped morphology through Gram staining. Hot spore staining revealed faint green endospores, affirming its spore-forming capability under nutrient-deprived conditions (*Supplementary 2*). A negative ring in the indole test (*Supplementary 2*) indicated its inability to break down tryptophan into indole, consistent with other *Bacillus* species. In the MR-VP test, the methyl red test was negative, indicating the absence of stable acidic end products, while the positive VP

test suggested the use of the butylene glycol pathway to produce neutral end products like acetoin (*Supplementary 2*).

### B. Iturin A Activity Identification & Extraction

The oil emulsification test confirmed the biosurfactant activity of Iturin A, with a zone of clearance observed when broth was added to petrol, pure Iturin A showed the highest emulsification activity. Iturin A was extracted from LB and PDB media for comparative analysis via HPLC, yielding 4 ml of filtered sample [10]. Results showed that PDB provided higher quantities of Iturin A (*Supplementary 2*).

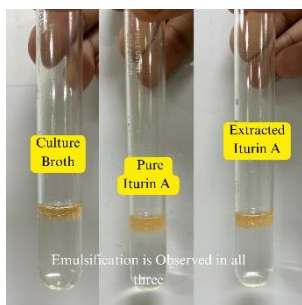


Fig 5: Oil Emulsification

### C. Growth Curve

Initial attempts to establish a 24-hour growth curve using a 100 µl inoculation did not yield distinct growth phases. Following optimization protocols provided by Dr. Sabari Sankar Thirupathy, a 1:1000 dilution and subsequent trials revealed diauxic growth patterns due to multiple sugars in LB medium. After sugar depletion, an exponential growth phase lasting three hours was observed before entering stationary phase.

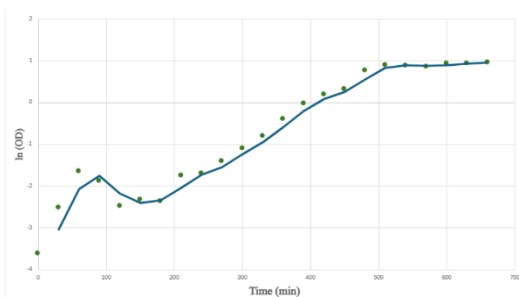


Fig 6: Growth Curve

### D. HPLC Analysis

HPLC analysis of extracted and pure Iturin A involved running standards at various concentrations, revealing multiple isomer peaks [11]. The calibration curve demonstrated linearity in peak area across concentrations [12].

The following chromatograms were obtained as a result of our HPLC runs.

#### 1) Standard Curve

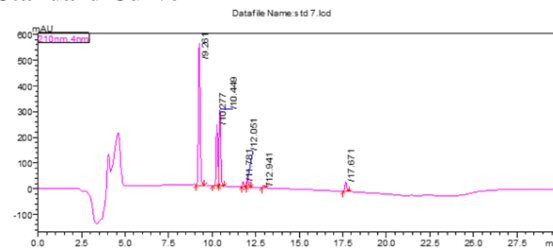


Fig 7: 100µg/ml Standard Curve

#### 2) Blank:

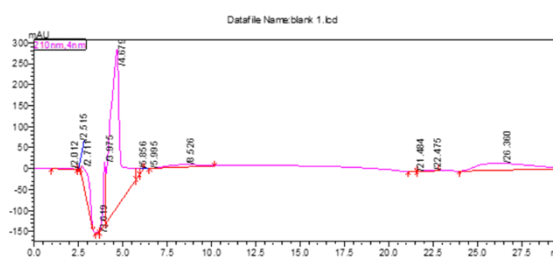


Fig 8: The graph shows the methanol peak, which was used as the blank since both our Iturin A standards and test samples were dissolved in methanol.

#### 3) Test samples:

- LB

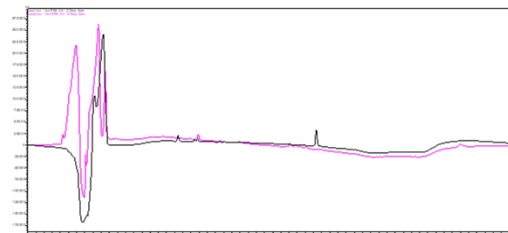


Fig 9: Comparison of the peaks between the extracted LB sample and the standard samples

- PDB

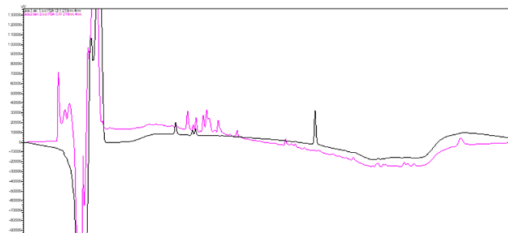


Fig 10: Comparison of the peaks between the extracted PDB sample and the standard samples

In the above graphs, black depicts standard chromatograms and pink depicts test sample chromatograms.

The Standard Curve (Cumulative Area vs Concentration) obtained is as follows:

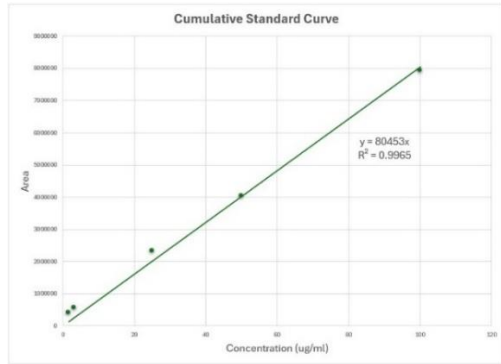


Fig 11: Standard Curve - Cumulative Area vs Concentration

The cumulative area for each test sample was calculated (Supplementary 2) and obtained as follows:

Table 2: Cumulative area as determined using HPLC for (a) PDB, (b) LB

Sample	Peak 1	Peak 2	Peak 3	Peak 4	Peak 5	Peak 6	Peak 7	Cumulative Area
PDB	14512	35229	82946	67258	14539	44585	9992	269061
Sample	Peak 1	Peak 2	Peak 3	Peak 4	Peak 5	Peak 6	Peak 7	Cumulative Area
LB	7196	9473	69523	13443	2835	9821	6174	118465

The concentration of Iturin A present in the sample extracted from cells grown in PDB is 3.344 $\mu$ g/ml while the concentration from cells grown in LB is 1.472 $\mu$ g/ml.

LB produced sharper peaks due to lesser media complexity and simpler composition.

### E. Fragment Amplification

Amplification results (Supplementary 2) showed successful amplification of the  $P_{bacA}$  fragment while the  $P_{43}$  fragment produced only faint bands. This discrepancy is attributed to suboptimal primer performance characterized by hairpin structures and low Gibbs free energy values. Future experiments will utilize more favorable primer combinations.

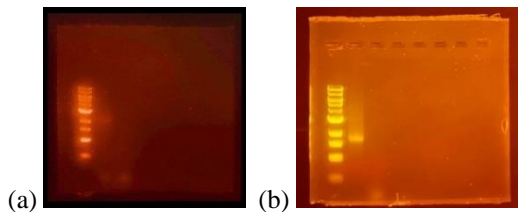


Fig 12: PCR Gel Results (a)  $P_{43}$ , (b)  $P_{bacA}$

### D. Homologous Recombination

Protocols for homologous recombination were optimized under guidance from Dr. Sabari (Supplementary 2). The selectable marker, GFP, allowed visualization of transformed colonies at an emission wavelength of 509 nm (Supplementary 2). Successful recombination with the  $P_{bacA}$  fragment resulted in clear green fluorescent colonies, whereas attempts with  $P_{43}$  were unsuccessful due to low amplification levels.

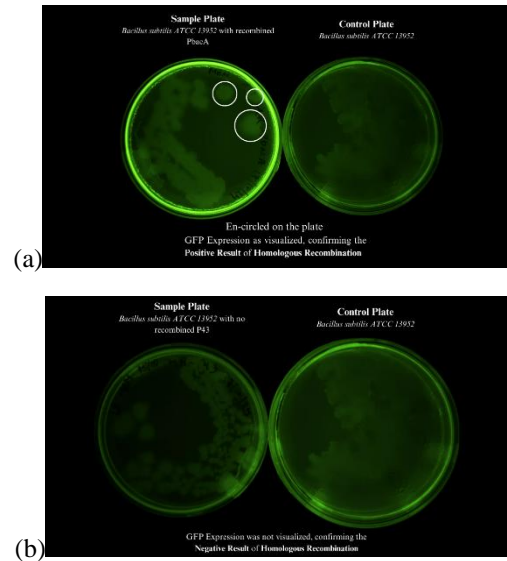


Fig 13: GFP Quantification results for HR, (a) Positive Result in  $P_{bacA}$ , (b) Negative result in  $P_{43}$

### IV. INFERENCES

Building on our success in demonstrating the efficiency of  $P_{bacA}$  within the proposed dual promoter solution and the successful quantification of Iturin A through HPLC analysis, the following key insights were identified to refine and enhance our experimental design.

The experiments revealed important understandings for future optimization. Increasing potassium L-glutamate concentration could enhance homologous recombination efficiency. In Iturin A extraction, PDB yielded higher concentrations, while LB provided sharper HPLC peaks due to its simpler composition. Weak amplification of the  $P_{43}$  fragment was attributed to suboptimal primer design, including issues like hairpin structures, primer dimers, and  $\Delta G$  values; the best primer combination, though selected, remained insufficient for strong amplification. HPLC chromatograms showed higher Iturin A concentration in PDB-extracted samples compared to LB, and calculations quantified Iturin A production under the natural promoter  $P_{itu}$ .

## V. MODELLING

A promoter's strength is primarily classified by the stability of its open complex and the binding affinity to the RNAP. Docking analyses were conducted to evaluate the interaction of sigma factors with the core regions of the  $P_{43}$  and  $P_{bacA}$  promoters, both in their unoptimized and optimized forms at the  $-10$  and  $-35$  regions. The goal was to determine whether optimization enhanced binding affinity to the sigma factors, which would indicate the potential for stronger gene expression. The  $-35$  and  $-10$  regions were changed to the predicted consensus sequence (*Supplementary 1*).

$P_{43}$  unoptimized and optimized core region fragments were docked with sigma factor A from its RNAP holoenzyme (PDB ID: 7ckq) and with sigma factor B whose structure was obtained from AlphaFold.  $P_{bacA}$  optimized and unoptimized core regions were docked with sigma factor B.

Table 3:  $P_{bacA}$  Unoptimized + Sigma B

Rank	1	2	3	4	5
Docking Score	-229.9	-227.8	-227.35	-225.14	-223.5
Confidence Score	0.8317	0.8259	0.8245	0.818	0.8131
Ligand RMSD (Å)	65.8	80.98	68.21	71.54	72.25

Table 4:  $P_{bacA}$  Optimized + Sigma B

Rank	1	2	3	4	5
Docking Score	-245.4	-225.8	-207.3	-204.87	-203.1
Confidence Score	0.8709	0.8202	0.759	0.7498	0.7431
Ligand RMSD (Å)	232.69	236.55	267.44	244.18	219.93

From the Docking scores it was inferred that optimizations made to  $P_{43}$  had no significant impact while  $P_{bacA}$  optimizations showed promising results and held grounds for future work (*Supplementary 1*).

Molecular Dynamics (MD) Simulation was carried out for the Protein-DNA complexes using the Gromacs v2024.1 software with AMBER99 forcefield for 100 ns time.

### A. Results:

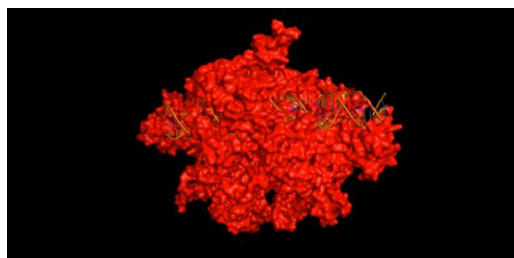


Fig 14:  $P_{bacA}$  Unoptimized interacting with SigB

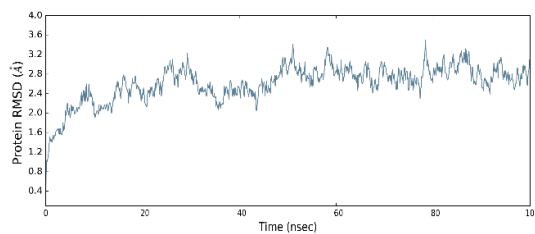


Fig 15: RMSD Values for  $P_{bacA}$  Unoptimized with SigB

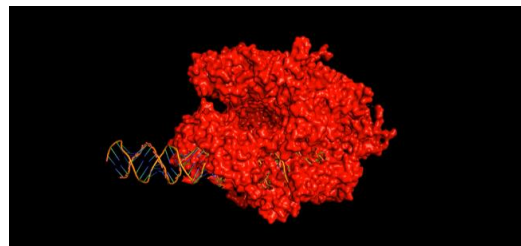


Fig 16:  $P_{bacA}$  optimized interacting with SigB

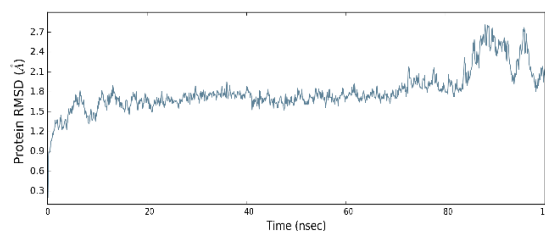


Fig 17: RMSD Values for  $P_{bacA}$  Optimized with SigB

The Root Mean Square Deviation (RMSD) of the Protein-DNA complexes illustrate that the optimized DNA-Protein complexes are more stable than the unoptimized complexes. All the RMSD graphs deviate within  $2 \text{ \AA}$ , which shows that all the complexes are stable (*Supplementary 1*). However, optimized complexes are more stable than unoptimized complexes. Optimized DNA exhibits better interactions with the protein compared to the unoptimized DNA.

## VI. FUTURE PROSPECTS

### A. Construction of $P_{43ca}$

Our design of the dual promoter aims to achieve continuous expression of Iturin A throughout the bacterial lifecycle, with induced surges upon fungal stress. We selected a constitutive promoter,  $P_{43}$ , and an inducible promoter,  $P_{bacA}$ , based on their expression characteristics in different phases of the *Bacillus* lifecycle [13].  $P_{43}$ , SigA and SigB dependent, is active primarily during the logarithmic phase, promoting Iturin A secretion, while  $P_{bacA}$ , SigB-dependent, responds during the stationary phase induced under stress. The primary promoter was chosen as  $P_{43}$  to maintain constant basal expression of Iturin A, while  $P_{bacA}$  was selected as the secondary promoter to induce expression during stress. This configuration avoids

excessive metabolic burden and ensures the efficient production of Iturin A.

The dual promoter arrangement was chosen due to the stated synergism between sigma A and sigma B promoters presumed to have better expression in the chosen orientation [14]. No spacer was added between the promoters as the upstream promoter element (UPE) of *P43* acts as a spacer, ensuring efficient RNA polymerase binding during the stationary phase as there is no interference among various promoter elements [15]. The inclusion of necessary regulatory regions, such as a suggested stringer RBS and 5' UTRs ensures the strength and functionality of both promoters, allowing for optimal Iturin A production throughout the bacterial lifecycle.

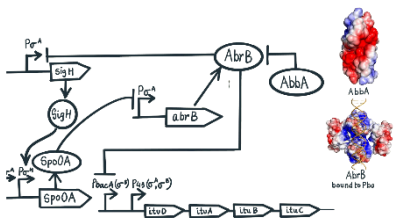


Fig 18: Regulatory pathways for Iturin production through the rearranged dual promoter.

## B. Implementation

The genetically modified *Bacillus subtilis* is used in wettable powder formulation. This eco-friendly, cost-effective biocontrol solution utilizes the dual promoter system for Iturin A production in our Biocontrol Agent (BCA), giving optimal results as both a preventive and curative measure contrary to traditional fungicides. Its stable, biodegradable formulation allows easy integration into standard agricultural practices.

## C. Composition and Formulation Breakdown

The six major components of the formulation including the BCA are incorporated using the following potential compounds as given below.

Table 5: Composition of Biocontrol Agent

Components	Possible Compound(s)	Role
<i>Bacillus subtilis</i> spores	(Supplementary 3)	Active ingredients provide antifungal activity.
Inert carriers	Silica (Aerogel), Calcium Carbonate (CaCO <sub>3</sub> ), Diatomite, Bentonite, Kaolin, Talc, Dextrin [16]	Ensures ease of application and mixing.

Dispersing agents	Sodium lignin sulfonate, Polyvinyl alcohol (PVA), Calgon, Sodium carboxymethyl cellulose (CMC-Na), Phosphate, Alkyl naphthalene sulfonate condensation polymer, Carboxylate macromolecule, Polycarboxylate polymeric modified resin, Alkyl sulfate, Polycarboxylate polymeric dispersant, Naphthalenesulfonate formaldehyde condensation compound, Alkylphenol polyoxyethylene formaldehyde condensate sulfonate, Microcrystalline cellulose [16], [17]	Facilitates proper suspension in water for spraying
Wetting Agents (Surfactants)	Tea saponin, Sodium Dodecyl Sulfate (SDS), Sodium dodecyl benzene sulfonate (SDB-Na), Naphthalene sulfonate (Morwet EFW), Sodium butyl naphthalene sulfonate, Lauryl sodium sulfate, Lignosulfonates, Isopropyl naphthalene sulfonate, Sodium alkyl aryl sulfonate, Tween 80 [16], [18]	Facilitates even dispersion, improves adhesion, reduces surface tension, and enhances coverage
Stabilizers	Calcium Carbonate CaCO <sub>3</sub> , Xanthan gum, K <sub>2</sub> HPO <sub>4</sub> , Lactose, Sodium benzoate, EDTA, Triethanolamine, Ammonium sulfate [16]	Prevents degradation, maintains suspension stability, and ensures shelf-life integrity
UV Protectants	VC (ascorbic acid) as the CMC (carboxymethyl cellulose), β-cyclodextrin, Oxybenzone, Blankophor BBH, Lignin (PC 1307) [16], [18]	shields active ingredients from UV degradation, enhancing stability and prolonging efficacy under sunlight.
Inducing agent	Methyl cumate powder [19]	Induces the kill-switch mechanism of the bacteria
Anti-caking agent	-	Prevents clumping during storage.

The estimated proportions of the wetting agent, stabilizer, and UV protectant will be determined after further experimentation and field testing.

## D. Production and Application

The production of wettable powder will focus on stability and field effectiveness. Spores will be cultured in bioreactors under optimized conditions, harvested, and dried using spray drying or lyophilizing to maintain viability. Additives will be dry mixed to create the formulation, followed by quality control checks for spore density, homogeneity, and storage stability. The final product will be packaged in moisture-resistant bags with proper labeling and storage instructions. Before use, the powder will be dispersed in water and applied using manual or

mechanical sprayers to ensure even distribution across coffee plant foliage.

The application will be done at the early stages of CLR detection or preventively before the rainy season, with increased frequency during high humidity or rainfall. Exact parameters, such as spore concentration and application frequency, will be determined through further experimentation and field studies. With proper application techniques and storage, the product offers long-term viability, environmental safety, and effectiveness in the field.

## VII. BIOSAFETY

Iturin A is a lipopeptide that has been shown to exhibit low toxicity and is considered safe for oral consumption. Studies have demonstrated that it causes no significant damage to vital organs such as the liver or small intestines while simultaneously enhancing probiotic availability in the gut. Additionally, it effectively reduces the population of harmful intestinal microflora, making it a promising compound for probiotic and gut health applications [20].

Iturin A also possesses insecticidal properties, with low lethal dosages against *Spodoptera litura* larvae, malarial insects, and other pests. Its mechanism of action involves inhibiting various gut proteases, thereby disrupting the digestive processes in insects [21].

### A. Kill Switch

To contain genetically modified *Bacillus subtilis* ATCC 13952, an inducible kill switch was proposed using *p*-isopropyl benzoate (Cumate) to regulate survival, causing cell death in its absence. The *galE* gene, encoding UDP-glucose 4-epimerase, is vital for metabolizing galactose in plant cell walls. Without *galE*, toxic intermediates accumulate, leading to cell death [19].

Key reactions catalyzed by UDP-glucose 4-epimerase: (i)  $\text{UDP-}\alpha\text{-D-glucose} \leftrightarrow \text{UDP-}\alpha\text{-D-galactose}$ ,

(ii)  $\text{UDP-N-acetyl-}\alpha\text{-D-glucosamine} \leftrightarrow \text{UDP-N-acetyl-}\alpha\text{-D-galactosamine}$ .

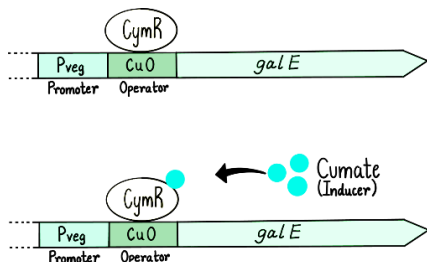


Fig 19: Cumate removes CymR repression, activating *galE* expression.

*GalE*'s natural promoter will be replaced with a synthetic cumate-inducible system combining the strong *Bacillus* promoter *P<sub>veg</sub>* and *Pseudomonas putida*'s CymR repressor. Cumate, included in a wettable powder sprayed on coffee leaves, will ensure antifungal activity against *H. vastatrix*. As Cumate degrades, the bacteria lose viability [19].

## VIII. HUMAN CENTERED DESIGN

CAAPI was a product of close interactions with our project stakeholders. The various steps that we adopted to determine our biocontrol agent, and our novel solution were a result of the team's efforts to connect with individuals and organizations outside of the team. Our team identified the project's stakeholders meticulously by answering questions pertaining to our project, enabling us to identify our stakeholders and integrate their viewpoints into our project. The team adopted a stakeholder-centric approach toward its efforts by creating a stakeholder map. The map classifies our key stakeholders into various subcategories for easy identification and to ensure all types of stakeholders are addressed in our project.

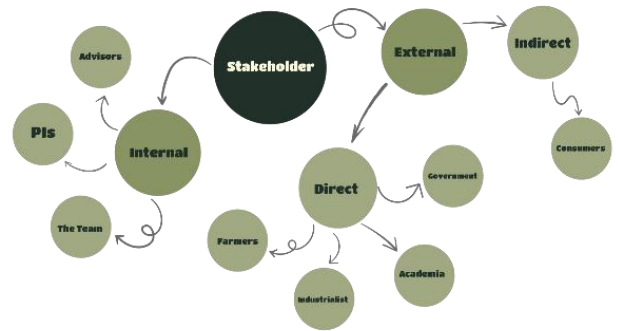


Fig 20: Stakeholder identification map for CAAPI

Our project is primarily centered around addressing our most important stakeholder, being the farmers who combat CLR through chemical fungicides. Our interactions with academicians who closely work with the CLR fungi enabled us to validate our synthetic biology approach involving a biocontrol agent, making it a better alternative to conventional fungicides. Speaking of coffee cultivators, they played a vital role in identifying the key problems faced in the coffee agricultural world. Apart from CLR itself, the uncertainty of coffee yields at the end of every harvest was identified as a noteworthy problem. Our software model was designed to keep this uncertainty in mind in hopes of alleviating this issue.

In response to these challenges, we developed a machine learning model named Bean Research and Estimate Workflow or BREW. This model utilizes data on various environmental factors—such as temperature, rainfall, soil moisture, and plantation area—sourced from databases like NATMO, IWRIS,



NASA, and the Coffee Board of India. The model employs advanced machine learning techniques, specifically a Random Forest algorithm, achieving an impressive  $R^2$  score of 0.986. This high level of accuracy enables farmers to predict yields better, optimize resource management, adapt to changing climatic conditions, and strengthen their market negotiation power.

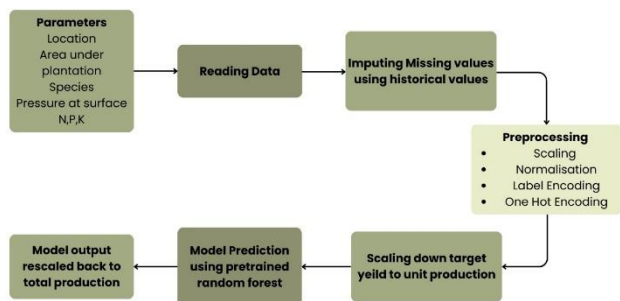


Fig 21: End-to-End Model Pipeline

Our project went beyond just interacting with farmers and academicians; we got the opportunity to interact with governmental bodies including the Coffee Board of India which helped our team identify potential ethical concerns with genetic modification of bacteria and further helped us develop our kill switch. Staying in touch with government bodies who themselves closely monitor agricultural activities helped us refine our future implementation strategies.

Our project mandated a strong human centered design approach considering it revolves around increasing the yield of the coffee plant and coffee being one of the most consumed beverages worldwide. We conducted surveys to understand the extent of understanding the public has about CLR. Despite widespread consumption of coffee, the knowledge about this fungal infection was not particularly prevalent. We considered this and tackled this by spreading awareness about this fungal infection in various institutional settings such as schools and universities. We specifically catered our content (*Supplementary 4*) towards various demographics during our educational drives across India giving our project a strong human centric base.

We felt like it was our responsibility to encourage other researchers to take up projects similar to ours to address concerns about farmers. For this, we designed and formulated handbooks about biopesticide formulations, promoter designing and stakeholder identification (*Supplementary 5*).

Overall, our human centered design was a two-way feedback system where we both gained information from the various stakeholders we connected with while also imparting knowledge to others about our work and this fungal infection.

## IX. CONCLUSION

Our project has successfully demonstrated the potential in enhancing an antifungal compound, in our case Iturin A which is naturally present in *Bacillus subtilis* to combat an adverse fungal infection caused in coffee called Coffee Leaf Rust without causing major environmental and ecological issues such as bioaccumulation and disrupting the microbiota of the coffee plantations. Using dry lab studies and research, we were able to develop the base work of our project by designing a suitable dual promoter system. Experimentation results such as HPLC, homologous recombination, and many other analytical techniques helped build our proof of concept. Throughout the development of project CAAPI – we kept our key stakeholders in mind addressing problems faced by them and integrating their input into our workflow.

However, this is just the beginning of developing a potent biocontrol agent with minimal repercussions and helping the farmers. With continued research, experimentation, and collaboration, we aim to advance this innovative solution into a scalable and sustainable biocontrol strategy, empowering farmers to combat Coffee Leaf Rust while preserving the ecological balance of their plantations.

## X. REFERENCES

- [1] M. Geissler, K. M. Heravi, M. Henkel, and R. Hausmann, "Lipopeptide Biosurfactants from Bacillus Species," *Biobased Surfactants: Synthesis, Properties, and Applications*, pp. 205–240, Jan. 2019, doi: 10.1016/B978-0-12-812705-6.00006-X.
- [2] C. R. Harwood, J. M. Mouillon, S. Pohl, and J. Arnau, "Secondary metabolite production and the safety of industrially important members of the Bacillus subtilis group," *FEMS Microbiol Rev*, vol. 42, no. 6, pp. 721–738, Nov. 2018, doi: 10.1093/FEMSRE/FUY028.
- [3] N. Roongsawang, K. Washio, and M. Morikawa, "Diversity of Nonribosomal Peptide Synthetases Involved in the Biosynthesis of Lipopeptide Biosurfactants," *International Journal of Molecular Sciences 2011, Vol. 12, Pages 141-172*, vol. 12, no. 1, pp. 141–172, Dec. 2010, doi: 10.3390/IJMS12010141.
- [4] R. Tsoi, F. Wu, C. Zhang, S. Bewick, D. Karig, and L. You, "Metabolic division of labor in microbial systems," *Proc Natl Acad Sci U S A*, vol. 115, no. 10, pp. 2526–2531, Mar. 2018, doi: 10.1073/PNAS.1716888115/SUPPL\_FILE/PNAS.1716888115.SAPP.PDF.
- [5] S. Mizumoto, M. Hirai, and M. Shoda, "Production of lipopeptide antibiotic iturin A using soybean curd residue cultivated with Bacillus subtilis in solid-state fermentation," *Appl Microbiol Biotechnol*, vol. 72, no. 5, pp. 869–875, Oct. 2006, doi: 10.1007/s00253-006-0389-3.
- [6] Y. Dang *et al.*, "Enhanced production of antifungal lipopeptide iturin A by Bacillus amyloliquefaciens LL3

- through metabolic engineering and culture conditions optimization,” *Microb Cell Fact*, vol. 18, no. 1, pp. 1–14, Apr. 2019, doi: 10.1186/S12934-019-1121-1/TABLES/3.
- [7] X. Li and W. D. Heyer, “Homologous recombination in DNA repair and DNA damage tolerance,” *Cell Research 2008 18:1*, vol. 18, no. 1, pp. 99–113, Jan. 2008, doi: 10.1038/cr.2008.1.
- [8] L. Krejci, V. Altmannova, M. Spirek, and X. Zhao, “Homologous recombination and its regulation,” *Nucleic Acids Res*, vol. 40, no. 13, p. 5795, Jul. 2012, doi: 10.1093/NAR/GKS270.
- [9] P. Bisicchia, E. Botella, and K. M. Devine, “Suite of novel vectors for ectopic insertion of GFP, CFP and IYFP transcriptional fusions in single copy at the amyE and bglIS loci in *Bacillus subtilis*,” *Plasmid*, vol. 64, no. 3, pp. 143–149, Nov. 2010, doi: 10.1016/J.PLASMID.2010.06.002.
- [10] T. J. P. Smyth, A. Perfumo, S. McClean, R. Marchant, and I. M. Banat\*, “Isolation and Analysis of Lipopeptides and High Molecular Weight Biosurfactants,” *Handbook of Hydrocarbon and Lipid Microbiology*, pp. 3687–3704, 2010, doi: 10.1007/978-3-540-77587-4\_290.
- [11] J. Yuan, W. Raza, Q. Huang, and Q. Shen, “Quantification of the antifungal lipopeptide iturin A by high performance liquid chromatography coupled with aqueous two-phase extraction,” *Journal of Chromatography B*, vol. 879, no. 26, pp. 2746–2750, Sep. 2011, doi: 10.1016/J.JCHROMB.2011.07.041.
- [12] J. Xiao, X. Guo, X. Qiao, X. Zhang, X. Chen, and D. Zhang, “Activity of Fengycin and Iturin A Isolated From *Bacillus subtilis* Z-14 on *Gaeumannomyces graminis* Var. *tritici* and Soil Microbial Diversity,” *Front Microbiol*, vol. 12, p. 682437, Jun. 2021, doi: 10.3389/FMICB.2021.682437/BIBTEX.
- [13] Y. Rao *et al.*, “Construction and application of a dual promoter system for efficient protein production and metabolic pathway enhancement in *Bacillus licheniformis*,” *J Biotechnol*, vol. 312, pp. 1–10, Mar. 2020, doi: 10.1016/J.JBIOTECH.2020.02.015.
- [14] T. Phanaksri, P. Luxananil, S. Panyim, and W. Tirasophon, “Synergism of regulatory elements in  $\sigma$ B- and  $\sigma$ A-dependent promoters enhances recombinant protein expression in *Bacillus subtilis*,” *J Biosci Bioeng*, vol. 120, no. 4, pp. 470–475, Oct. 2015, doi: 10.1016/J.JBIOSEC.2015.02.008.
- [15] C. A. Klein, M. Teufel, C. J. Weile, and P. Sobetzko, “The bacterial promoter spacer modulates promoter strength and timing by length, TG-motifs and DNA supercoiling sensitivity,” *Scientific Reports 2021 11:1*, vol. 11, no. 1, pp. 1–13, Dec. 2021, doi: 10.1038/s41598-021-03817-4.
- [16] H. CHENG, L. LI, J. HUA, H. YUAN, and S. CHENG, “A Preliminary Preparation of Endophytic Bacteria CE3 Wettable Powder for Biological Control of Postharvest Diseases,” *Not Bot Horti Agrobot Cluj Napoca*, vol. 43, no. 1, pp. 159–164, May 2015, doi: 10.15835/nbha4319699.
- [17] “CN104365592A - *Trichoderma* wettable powder and preparation method thereof - Google Patents.” Accessed: Jan. 15, 2025. [Online]. Available: <https://patents.google.com/patent/CN104365592A>
- [18] D. A. Schisler, P. J. Slininger, R. W. Behle, and M. A. Jackson, “Formulation of *Bacillus* spp. for Biological Control of Plant Diseases,” *Phytopathology*, vol. 94, no. 11, pp. 1267–1271, Nov. 2004, doi: 10.1094/PHYTO.2004.94.11.1267.
- [19] A. Klotz, A. Kaczmarczyk, and U. Jenal, “A Synthetic Cumate-Inducible Promoter for Graded and Homogenous Gene Expression in *Pseudomonas aeruginosa*,” *Appl Environ Microbiol*, vol. 89, no. 6, Jun. 2023, doi: 10.1128/AEM.00211-23/SUPPL\_FILE/AEM.00211-23-S0010.MP4.
- [20] H. Zhao *et al.*, “Potential of iturins as functional agents: safe, probiotic, and cytotoxic to cancer cells,” *Food Funct*, vol. 9, no. 11, pp. 5580–5587, Nov. 2018, doi: 10.1039/C8FO001523F.
- [21] N. K. Papatthoti, D. Kiddeejing, J. R. Daddam, T. Le Thanh, and N. Buensanteai, “Identification of Protease Inhibition Mechanism by Iturin A against Agriculture Cutworm (*Spodoptera litura*) by Homology Modeling and Molecular Dynamics,” *Open Bioinform J*, vol. 13, no. 1, pp. 119–128, Dec. 2020, doi: 10.2174/1875036202013010119.